Backscattering from a rough, high dielectric constant surface: an application for radar sensing of ocean clutter

Jojit C. Torcedo*, Thomas M. Goyette, and Andrew J. Gatesman

Submillimeter-Wave Technology Laboratory, University of Massachusetts Lowell, Lowell, MA 01854

ABSTRACT

Physical scale modeling of the electromagnetic backscatter behavior of static sea states using dielectric models and indoor compact radar ranges has the potential to offer a unique and advantageous method to probe ocean scattering phenomenology not feasible using conventional radar measurements on dynamic sea surfaces. As an initial step towards developing such modeling techniques, the millimeter-wave backscatter of a static, simplified rough surface made from a material that electromagnetically models the X-band dielectric properties of seawater has been measured. Computational electromagnetic modeling of the surface was performed using Xpatch and is compared with compact range measurements. By starting with simplified sea-state surfaces, the aim is to develop a reliable scale modeling approach capable of studying the backscattering behavior of realistic ocean surfaces.

Keywords: Dielectric, millimeter wave, terahertz, water, ocean clutter, backscatter

1. INTRODUCTION

Since the very early days of radar, the scattering properties of the ocean surface has been the subject of numerous investigations over the decades. The scattering cross section of the sea can be affected by several uncontrollable and dynamic environmental factors – wind direction, wind speed, wave height, and wave direction – making it difficult to determine its relationship to wavelength, elevation angle, and polarization.[1] For this reason, a compact radar range measurement utilizing $1/16^{th}$ physical scale modeling techniques in a controlled laboratory environment can be an advantageous method for understanding the radar scattering of sea surfaces. For example, for a given sea state, a full investigation of its backscattering behavior can be probed as a function of frequency, elevation angle, azimuth angle, and polarization. Such a thorough investigation would not be possible by studying an actual dynamic ocean surface. However, a material that accurately models the radar band dielectric properties of seawater at millimeter wavelengths has yet to be reported in the literature. Therefore, the aim of this work was to develop a specially formulated artificial dielectric material that electromagnetically models the X-band (10 GHz) dielectric properties of seawater at $1/16^{th}$ scale (160 GHz). Furthermore, compact radar range ISAR imagery on a periodically rough surface made from this material was collected at various elevation angles and the backscatter coefficient determined. Finally, Xpatch simulation results are presented and compared to the measurements.

*jojit_torcedo@uml.edu; phone 1 978 934-1300; fax 1 978 452-3333; stl.uml.edu

1.1 The microwave complex dielectric constant (CDC) and front surface reflectivity of seawater

In 2004, Meissner and Wentz[2] compiled data from numerous sources and fit the microwave CDC of water in the salinity range between 0 – 40 parts per trillion (ppt). The double Debye relaxation model showed good agreement and is shown in Figure 1, where the real and imaginary parts of the CDC for seawater (35 ppt salinity) at 0, 15, and 30 degrees C are plotted between 2 – 40 GHz. Figure 2 shows the corresponding front surface reflectivities of seawater. The Meissner and Wentz work served as a guide for the development of a scaled dielectric to simulate the microwave properties of water at millimeter wavelengths.

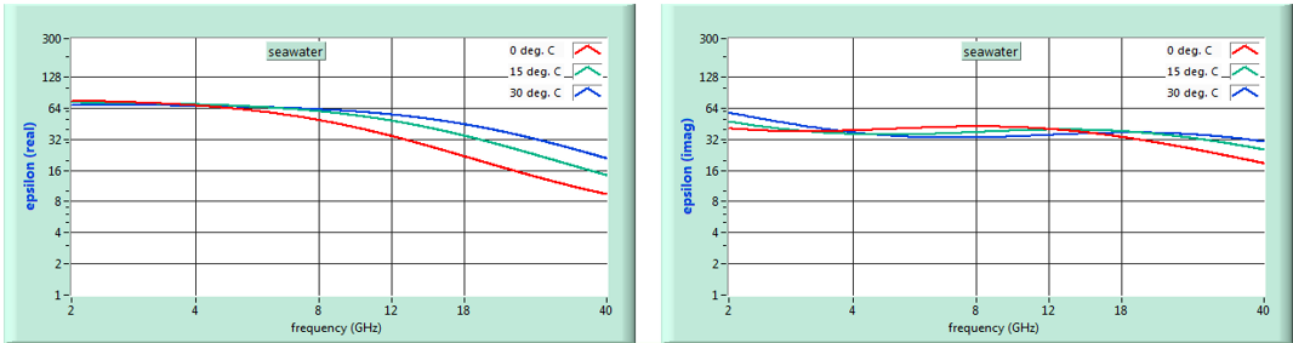

Figure 1. Real part of CDC (left) and imaginary CDC (right) for seawater at 35 ppt salinity at 0, 15, and 30 deg. C.[2]

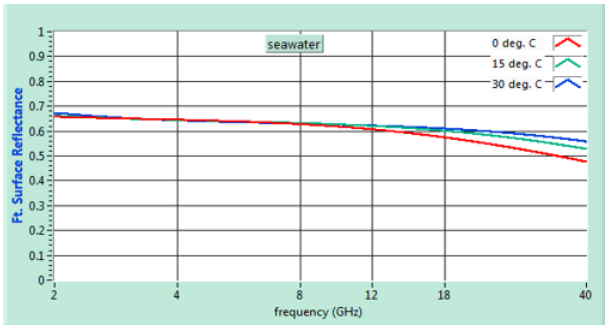

Figure 2. Front surface reflectivity of seawater at 35 ppt salinity at 0, 15, and 30 deg. C.[2]

2. ARTIFICIAL DIELECTRICS

2.1 Fabrication of the periodically rough surface

The periodically rough plate was composed of -200 mesh aluminum (Al) powder (>99%) and a two-part polyurethane elastomer resin, Smooth Cast 326 (SC326), both obtained from Smooth-On, Inc. SC326 was chosen for its low viscosity (100 cps) and capability of supporting large Al powder loading amounts while remaining fluid to easily cast into the silicone mold. Additionally, SC326 has a relatively short pot life of 7-9 minutes to mitigate against Al particle settling (yet long enough to thoroughly mix).

The mass of Al powder added to the mixture for a desired loading percentage was calculated by using common baker's percentages:

$$m_{Al} = m_{SC326} \times (\%loading) \tag{1}$$

SC326 is a two-part polyurethane resin with a mixing ratio of 1:1 by volume (115A:100B by mass). A mass of 708 g of part A and 616 g of B were dispensed in separate 5 gallon buckets. Through extensive studies of several Al powder loading amounts in SC326, it was determined that a loading percentage of 197% was the most appropriate for modeling the X-band dielectric properties of seawater at 1/16th scale. The mass of Al powder was calculated using the simple formula above, resulting in 1395 g and 1214 g of Al powder being added to parts A and B, respectively. The powder

loaded A and B resins were thoroughly mixed to eliminate any clumps, and were degassed in a vacuum chamber at -30 inHg for ~5 minutes to remove air bubbles. The loaded A and B resins were then combined in a third bucket which was stirred for about 2 minutes to achieve thorough mixing and ensure complete curing. The A+B mixture was then degassed for 2 minutes, brought back to atmosphere, and gently mixed (rolled) for 2 additional minutes to ensure homogenous distribution of Al powder. The mixture was then poured into a silicone mold and allowed to cure for 12 hours prior to de-molding. After curing, the plate was mounted on a low radar cross section pylon in a 160 GHz compact range for backscatter measurements (Figure 3). The plate measures 20" x 13.75", the valley-to-peak height of the periodic surface is 7.5 mm, and the periodicity along the long edge is 25.4 mm and 17.4 mm along the short edge.

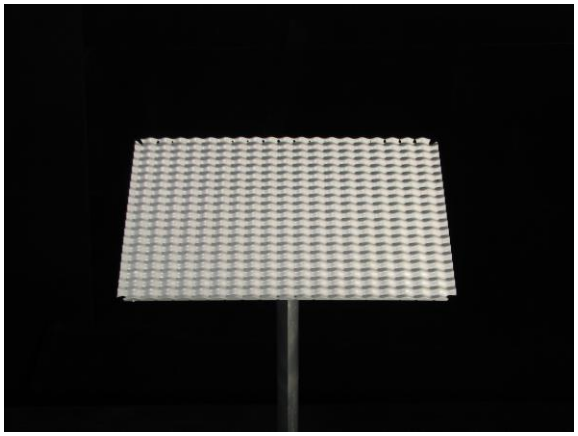

Figure 3. Photograph of the periodically rough plate made of an Al powder loaded polyurethane polymer mixture.

It should be noted that the master from which the plate in Figure 3 was molded was a metal, periodically rough plate originally fabricated for an unrelated project. The master plate was chosen for this work since its periodic surface lends itself to predictable Xpatch simulation results, and its valley-to-peak height is ~ 1/16th that of actual ocean wave heights[10].

2.2 Reflectance and CDC measurements

In addition to the periodic plate, small samples of Al loaded polymer were also cast into 1.5" diameter cylindrical molds for reflectance and CDC characterization. Reflectance measurements at 11 degrees incidence and normal incidence transmittance measurements were made between 5 – 55 wavenumbers on a Bruker 80v FTIR spectrometer and are shown in Figure 4. Reflectance and transmittance samples were 0.25" and 0.010" thick, respectively. The CDC was determined by using the standard method of fitting the transmittance spectra to the Fresnel equations[8].

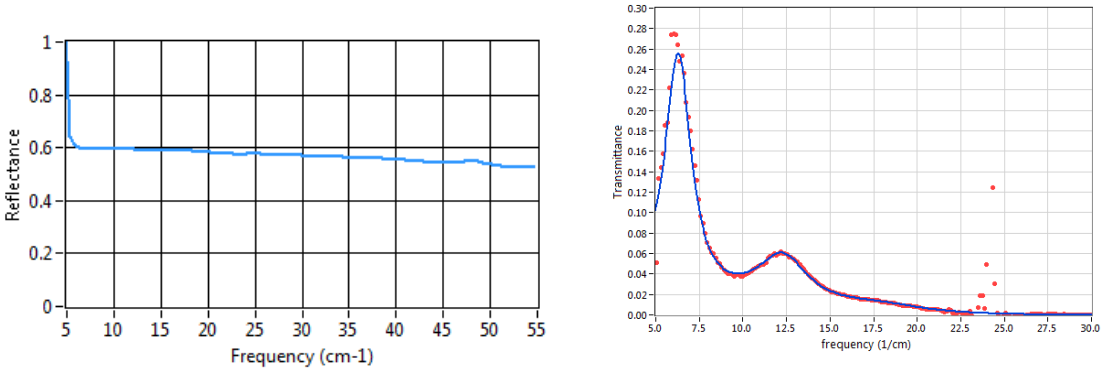

Figure 4. FTIR reflectance spectrum (left) and transmittance spectrum (right). The red dots in the transmittance spectrum are the measured points, the blue line is the Fresnel equation fit.

The CDC, determined from the fit of the transmittance spectra, was $\varepsilon = 69.79 + 12.19i$, which yields a front surface reflectivity of 0.621 at 160 GHz. The front surface reflectivity agrees well with the measured 160 GHz reflectance of 0.638.

2.3 Reflectivity comparison of seawater at X-band and artificial dielectric at 160 GHz

The theoretically predicted reflectivity of seawater (15 degrees C, 35 ppt salinity) and 197% Al loaded SC326 between 0° – 90° angle of incidence at s-polarization and p-polarization states were compared. As shown below, the reflectivity of 197% Al loaded SC326 at 160 GHz closely follows the general optical behavior of sea water at 10 GHz, with a delta of only 0.03, despite the obvious discrepancy in the CDC shown in Table 1.

Table 1. Comparison of front surface reflectivity and CDC for seawater and Al loaded SC326

	Frequency (GHz)	**Front Surface Reflectivity**	**Real ε**	**Im ε**
Seawater (15 ºC, 35 ppt salinity)[2]	10	0.625	53.46	38.67
Al loaded SC326	160	0.621	69.79	12.19

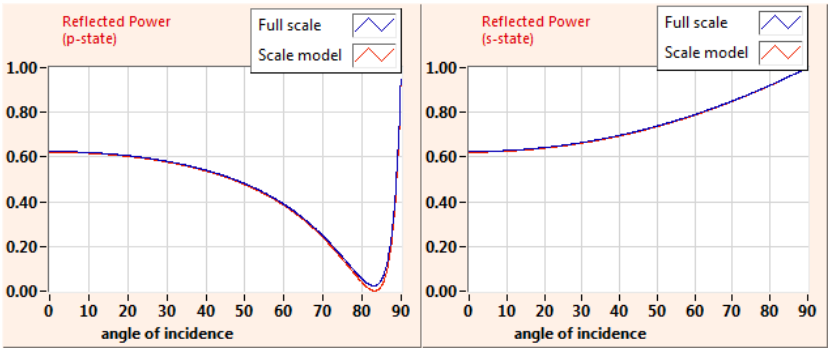

Figure 5. Reflectivity plots of p-polarization and s-polarization for seawater ("full scale," blue) and Al loaded SC326 ("scale model," red).

3. ISAR MEASUREMENTS

ISAR imagery was acquired at 160 GHz for the periodically rough plate shown in Figure 3 utilizing a fully polarimetric compact radar range; a description of the range can be found in the literature[3]. Each pixel of the ISAR image corresponds to a specific position on the material under test and effectively gives the RCS of the rough surface at that location. By summing the RCS of each pixel in a user selected area, the total RCS within the selected area was obtained. The backscatter coefficient σ^0 can then be determined by dividing the total RCS by the selected area. By calculating σ^0 in this manner, we can eliminate scattering contributions from the plate edge or the mounting pylon[4,9]. Imagery was obtained at elevation angles between 5° to 75° at 5° intervals. The σ^0_{HH} and σ^0_{VV} values reported at each elevation angle are averaged over azimuthal angles between 0° - 360°.

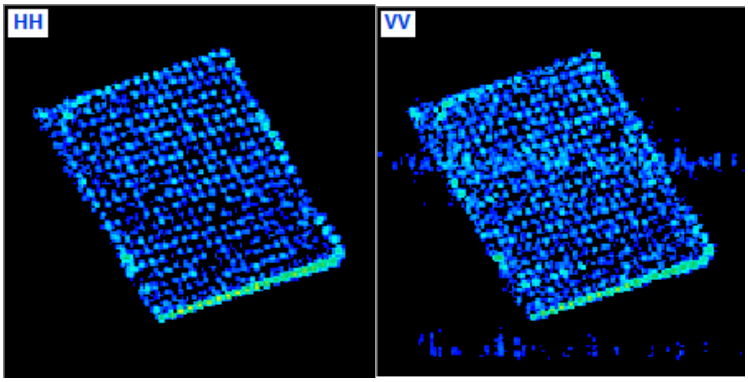

Figure 6. HH and VV ISAR image of periodically rough plate at 40° elevation angle.

3.1 Backscatter Measurements

Presented in Figure 7 is a plot of the average σ^0_{HH} and σ^0_{VV} as a function of elevation angle. For angles between 5° and 40°, σ^0_{VV} is larger while for elevation angles > 40°, σ^0_{HH} and σ^0_{VV} are nearly identical. Furthermore, there is a distinct inflection point in the graph at 40° where σ^0 rapidly increases with elevation angle. This behavior of σ^0 as a function of elevation angle has also been observed in X-band field measurements of seawater[1,5]. In general, the backscattering behavior as a function of elevation angle of a rough surface (both dry ground and sea) can be divided into three regions: low elevation angles, a plateau region, and high elevation angles[7,9]. The σ^0 behavior observed for the periodically rough plate clearly agrees with field measurements in the literature with a distinct plateau region (5° – 40°) and a high elevation angle region (>40°). It is important to note the second plateau region that was observed for high elevation angles between 55° – 75°. The upper plateau reported for the X-band backscatter of seawater in the literature is somewhat narrower, where σ^0 appears to have a second inflection point and level out at ~80° elevation angle[1].

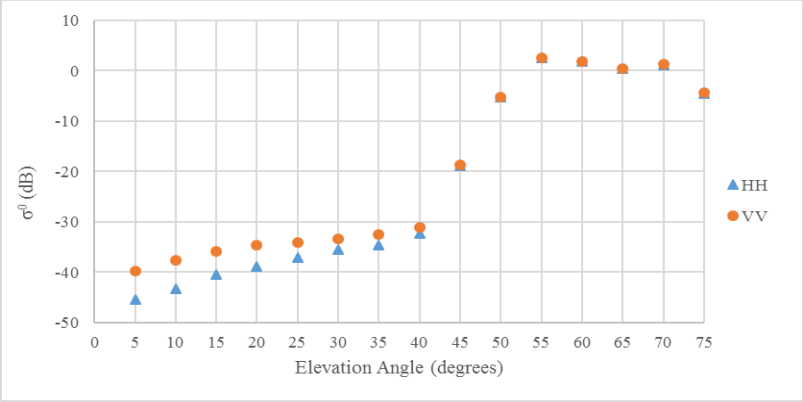

Figure 7. σ^0 versus elevation angle of from measured ISAR imagery

In the lower plateau region of Figure 7, σ^0_{VV} is larger throughout, with a ~5 dB difference between σ^0_{HH} and σ^0_{VV} at 15°, decreasing to ~2.5 dB at 40°. Previous field measurements on the X-band backscatter of seawater have shown this same polarimetric behavior[1,5,6].

4. XPATCH SIMULATIONS

A CAD model of the periodically rough plate was generated in Solidworks and imported into Xpatch to generate simulated ISAR imagery at 160 GHz. The dielectric properties of the simulation were set to the measured CDC of Al loaded SC326. Xpatch computed the ISAR imagery for elevation angles between 5° – 70°. From the simulated ISAR images, σ^0 was then calculated by using the same procedure described above for the measured ISAR data.

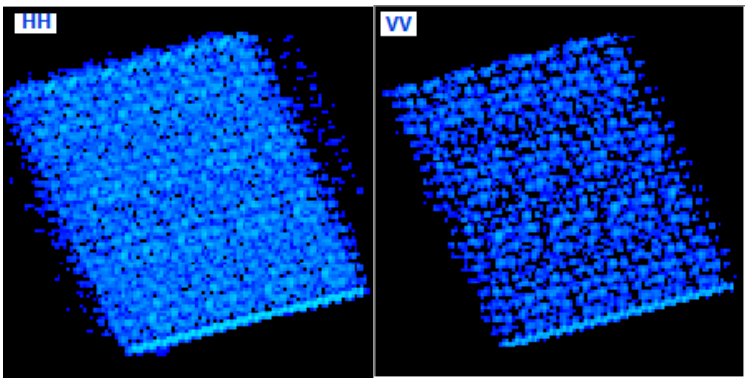

Figure 8. HH and VV Xpatch simulated ISAR images at 40 degrees elevation angle.

The σ^0 as a function of elevation angle derived from Xpatch simulated ISAR images is presented in Figure 9. A clear plateau and high elevation angle region was observed in the simulation. Interestingly, for elevation angles at 55° and above, σ^0 stays relatively flat and no longer increases, similar to what was observed in the 160 GHz ISAR measurements. However, in the lower plateau region, σ^0_{HH} is slightly larger than σ^0_{VV} by ~ 2 dB, where the measured σ^0 exhibited the opposite behavior. Despite the fact that the X-band σ^0_{VV} of seawater is typically larger than σ^0_{HH} [1,5,6], this does not necessarily disagree with the literature as $\sigma^0_{HH} > \sigma^0_{VV}$ was observed for X-band measurements in the circumstance of "very rough seas"[1].

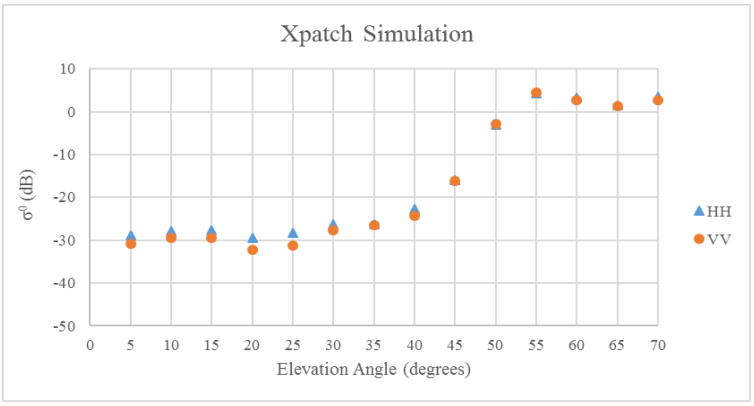

Figure 9. σ^0 versus elevation angle of from Xpatch simulated ISAR imagery

Shown in Figure 10 below is a comparison of the measured and simulated σ^0 for HH and VV polarizations. Overall, the simulated σ^0 is larger than the measured, with the smallest differences being in the high elevation angle region of the data. The simulated Xpatch data also show inflection points at 40° and 55° elevation angles, just as the measured ISAR data did. In addition, the simulated Xpatch σ^0 shows better agreement with the measured values for VV polarization.

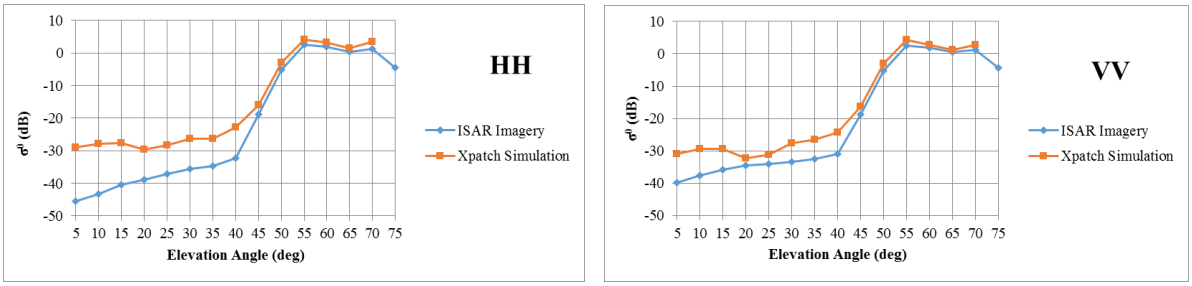

Figure 10. Comparison of measured and simulated σ^0.

5. CONCLUSION

The development of an artificial dielectric that closely models the reflectivity of water at X-band achieved. A periodically rough plate made from this newly developed material was fabricated, ISAR imagery as a function of elevation angle and polarization was acquired, and the backscattering properties were investigated. The σ^0 measurements at 160 GHz show reasonable agreement with the X-band backscattering behavior of seawater from the literature. Xpatch simulations were also performed and showed similar inflection points of σ^0 as a function of elevation angle, but differed in the polarimetric behavior in the lower plateau region. This study serves to set the basis for future 1/16th scale investigations of σ^0 at other frequency bands, wave heights, and of more complicated and realistic sea surfaces.

REFERENCES

[1] M. W. Long, R. D. Wetherington, J. L. Edwards, A. B. Abeling, "Wavelength Dependence of Sea Echo," Final Report, Georgia Institute of Technology (1965).

[2] T. Meissner, F. J. Wentz, "The Complex Dielectric Constant of Pure and Sea Water from Microwave Satellite Observations," Vol 42, No. 9, Sept. 2004.

[3] M. J. Coulombe et al., "A 160 GHz polarimetric compact range for scale model RCS measurements," in Proc. AMTA, vol. 239. 1996, pp. 239-244.

[4] D. A. DiGiovanni, A. J. Gatesman, R. H. Giles, and W. E. Nixon, "Backscattering of Ground Terrain and Building Materials at Millimeter-Wave and Terahertz Frequencies," in Passive and Active Millimeter-Wave Imaging XVI, edited by David A. Wikner, Arttu R. Luukanen, Proceedings of SPIE Vol. 8715, June 2013.

[5] Goldstein, H. "Sea Echo," in Propagation of Short Radio Waves, edited by Kerr, D. E., MIT Radiation Laboratory Series, McGraw-Hill, New York, 499-514 (1951).

[6] Cowan, E. W., RL Report No. 870, Jan. 10 1946.

[7] Beckman, P., [The Scattering of Electromagnetic Waves from Rough Surfaces], The MacMillan Company, New York, pp. 400-401 (1963).

[8] R. M. A. Azzam, N. M. Bashara, [Ellipsometry and Polarized Light], North-Holland, Amsterdam, pp. 269-288 (1977).

[9] A. J. Gatesman, T. M. Goyette, J. C. Dickinson, R. H. Giles, J. Waldman, J. Sizemore, R. M. Chase, W. E. Nixon, "Polarimetric Backscattering Behavior of Ground Clutter at X, Ka, and W-band," Proc. SPIE Vol. 5808, pp. 428-439, Algorithms for Synthetic Aperture Radar Imagery XIII; Edward G. Zelnio, Frederick D. Garber; Eds. May 2005.

[10] W. L. Jones, L. C. Schroeder, J. L. Mitchell, "Aircraft Measurements of the Microwave Scattering Signature of the Ocean," IEEE Transactions On Antennas and Propagation, Vol. 25, No. 1, January 1977.